

Article

Paleoenvironmental and Bio-Sequence Stratigraphic Analysis of the Cretaceous Pelagic Carbonates of Eastern Tethys, Sulaiman Range, Pakistan

Shuja Ullah ^{1,*}, Irfan U. Jan ¹, Muhammad Hanif ¹, Khalid Latif ¹, Mohibullah Mohibullah ², Mahnoor Sabba ¹, Aqsa Anees ³ , Umar Ashraf ³  and Hung Vo Thanh ^{4,*} 

¹ National Centre of Excellence in Geology, University of Peshawar, Peshawar 25120, Pakistan; irfan_nceg@uop.edu.pk (I.U.J.); mhanif_nceg@uop.edu.pk (M.H.); khalidlatif@uop.edu.pk (K.L.); mahnoorsabba57@gmail.com (M.S.)

² Department of Geology, University of Baluchistan, Quetta 87300, Pakistan; mohibullah.kakar@um.uob.edu.pk

³ Institute for Ecological Research and Pollution Control of Plateau Lakes, School of Ecology and Environmental Science, Yunnan University, Kunming 650504, China; aqsaanees01@outlook.com (A.A.); umarash2010@hotmail.com (U.A.)

⁴ School of Earth and Environmental Sciences, Seoul National University, Seoul 08826, Korea

* Correspondence: shujageo@gmail.com or shuja_nceg@uop.edu.pk (S.U.); vothanhhung198090@gmail.com (H.V.T.)



Citation: Ullah, S.; Jan, I.U.; Hanif, M.; Latif, K.; Mohibullah, M.; Sabba, M.; Anees, A.; Ashraf, U.; Vo Thanh, H. Paleoenvironmental and Bio-Sequence Stratigraphic Analysis of the Cretaceous Pelagic Carbonates of Eastern Tethys, Sulaiman Range, Pakistan. *Minerals* **2022**, *12*, 946. <https://doi.org/10.3390/min12080946>

Academic Editors:
Marianna Kulkova
and Dmitry Subetto

Received: 8 June 2022

Accepted: 26 July 2022

Published: 27 July 2022

Publisher's Note: MDPI stays neutral with regard to jurisdictional claims in published maps and institutional affiliations.



Copyright: © 2022 by the authors. Licensee MDPI, Basel, Switzerland. This article is an open access article distributed under the terms and conditions of the Creative Commons Attribution (CC BY) license (<https://creativecommons.org/licenses/by/4.0/>).

Abstract: The Cretaceous pelagic carbonate succession, i.e., Goru Formation was studied in the Chutair Section, Sulaiman Range, representing part of the eastern Tethys for the paleoenvironment and bio-sequence stratigraphy. Eight planktonic foraminiferal biozones are identified which include: 1. *Muricohedbergella planispira* Interval Zone; 2. *Ticinella primula* Interval Zone; 3. *Biticinella breggiensis* Interval Zone; 4. *Rotalipora appenninica* Interval Zone; 5. *Rotalipora cushmani* Total Range Zone; 6. *Whiteinella archeocretacea* Partial Range Zone; 7. *Helvetoglobotruncana helvetica* Total Range Zone; and 8. *Marginotruncana sigali* Partial Range Zone representing Albian-Turonian age. The petrographic studies revealed five microfacies: 1. Radiolarians-rich wacke-packestone microfacies; 2. Radiolarians-rich wackestone microfacies; 3. Planktonic foraminiferal wacke-packestone microfacies; 4. Planktonic foraminiferal wackestone microfacies; and 5. Planktonic foraminiferal packestone microfacies; indicating deposition of the Goru Formation in outer-ramp to deep basinal settings. Based on the facies variations and planktonic foraminiferal biozones, the 2nd and 3rd order cycles are identified, which further include six transgressive and five regressive system tracts. The sea level curve of the Goru Formation showed fluctuation between outer-ramp and deep-basin, showing the overall transgression in the 2nd order cycle in the study area, which coincides with Global Sea Level Curve; however, the 3rd order cycle represents the local tectonic control during deposition of the strata.

Keywords: microfacies; biostratigraphy; Chutair Section; sequence stratigraphy; Sulaiman Range; Stratigraphic Analysis; eastern Tethys

1. Introduction

The Sulaiman Range in Pakistan consists of thick Triassic to Pleistocene sedimentary succession [1,2]. Whilst these units represent predominantly marine succession, the post Eocene shows the fluvial depositional realms [2]. Among all marine succession, the pelagic carbonates of the Goru Formation, which is subject of the current study, was deposited in the Cretaceous time (i.e., mid-Cretaceous) [3]. The Early and Early Late Cretaceous reflect a period of significant paleoenvironmental changes, which manifested itself in the installation of widespread dys-aerobic to anaerobic conditions in outer-shelf and basinal settings on multiple stages [4,5]. The mid-Cretaceous period (i.e., 124–90Ma) saw a shift in the ocean-climate system's dynamic. Increased tectonic activity and changing paleogeography were

responsible for the changes [6]. The planktons preserved in deep-sea marl, organic-rich shale, and pelagic carbonate from the mid-Cretaceous (Barremian–Turonian) period provide an important record of how the marine biosphere responded to short- and long-term changes in the ocean-climate system [7]. Dynamic paleo-oceanographic settings affected the evolution of planktonic foraminifera throughout the mid-Cretaceous [8]. A vital radiation in the evolution of planktonic foraminifera occurred during the Late Albian–Cenomanian (105–93 Ma), characterised by the appearance of new morphologies, such as single-keeled trochospiral and biserial taxa with supplementary apertures, and the development of complex wall textures, such as macroperforate, muricate, and costellate, which lasted until the end of the Cretaceous [9]. The mid-Cretaceous, in the marine plankton, was likewise a time of high radiation and turnover [10]. The southern high latitudes were likely the main sources of deep-water production during the mid-Cretaceous, with subtropical convection restricted to isolated basins [11].

The autotrophic calcareous nano-plankton and heterotrophic planktonic foraminifera and radiolarians, both of which have mineralized skeletons of calcium carbonate and silica, are both abundant and well-preserved in mid-Cretaceous marine strata [7]. At or near the Oceanic Anoxic events (OAEs), radiolarians show high rates of evolutionary turnover that is extinction and radiation [12]. During the Cenomanian–Turonian boundary, the first bioevent occurred and the isochronous extinction of rotaliporids and the evolution/diversification of *Praeglobotruncana*, *Dicarinella*, and *Marginotruncana* indicate the start of the Turonian [7,13,14].

Based on planktonic foraminifera biostratigraphy, the pelagic carbonates of the Goru Formations in the Southern Kirthar Ranges represent Cretaceous age and the fauna show an open-marine environment [15]. The Goru Formation in the Lower Indus Basin (i.e., Kirthar Ranges) comprised of yellowish to greenish grey, fine to coarse grain sandstone interbedded with siltstone and shale in lower part whilst dark gray-to-black shales with siltstone and clay interbeds in upper part [16,17]. Here, the Goru Formation represents the main hydrocarbon bearing reservoir zone [18–21]. Previously researchers have conducted only patchy work on the Goru Formation in the Lower Indus Basin with respect to deposition and biostratigraphy; authors in a study [22] assigned the Albian to Cenomanian age to the Goru Formation on the Nar River Section, near Goru village in the Kirthar Range. In another study, authors [23] assigned to it Albian to Cenomanian age based on calcareous nannofossils and planktonic foraminifera of NW Pakistan. The Goru Formation in the Kirthar Range was allotted as an Lower Aptian to Coniacian age [24]. The Goru Formation has not been studied in detail in the study area for biostratigraphy, paleoenvironments and sequence stratigraphy. Therefore, the aims of this study are to determine the biostratigraphy, paleoenvironments and sequence stratigraphy of the Goru Formation.

2. Tectonic and Stratigraphic Settings

The Sulaiman Range is a structurally and tectonically active thin-skinned fold and thrust belt that developed from an oblique collision between Eurasia and India [25]. The Chaman sinistral strike slip fault and the Zhob Ophiolites (i.e., Muslim Bagh Ophiolites) form the northern and western boundaries of this thrust belt (Figure 1). It resulted by transpression of left lateral Chaman Fault as well as the southward thrusting of the western end of the India [26–28]. The Sulaiman Range has a Triassic to Oligocene stratigraphy. The Chutair Section is a part of the Sulaiman Range near Ziarat. The stratigraphic succession exposed in the study area ranges from the Triassic Wulgai Formation to the Oligocene conglomerate [3] (Figure 2), having being deposited on a broad shelf opening in the westward terminations into the southerly expansion of the Tethys during the Early Cretaceous [3]. The Goru Formation in the western part of the Sulaiman Range, where the study area is located, is primarily composed of thinly bedded limestone. The limestone has a grey hue in the lower part of the formation, a cream color in the middle, and a red and brown color in the upper part (Figure 2).

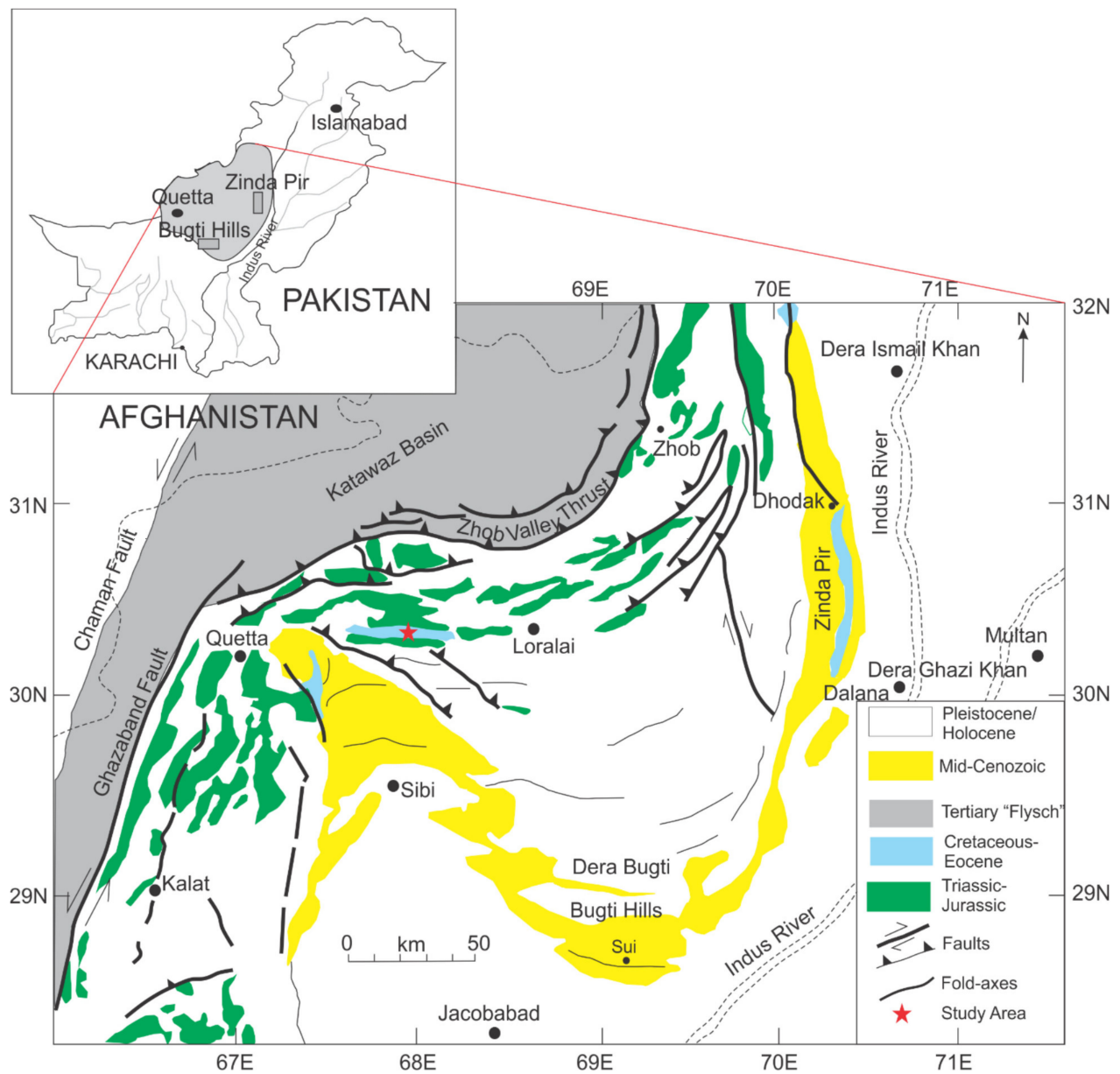


Figure 1. Map showing the study area and distribution of Triassic to Holocene rocks in the Sulaiman Range. (After [29]).

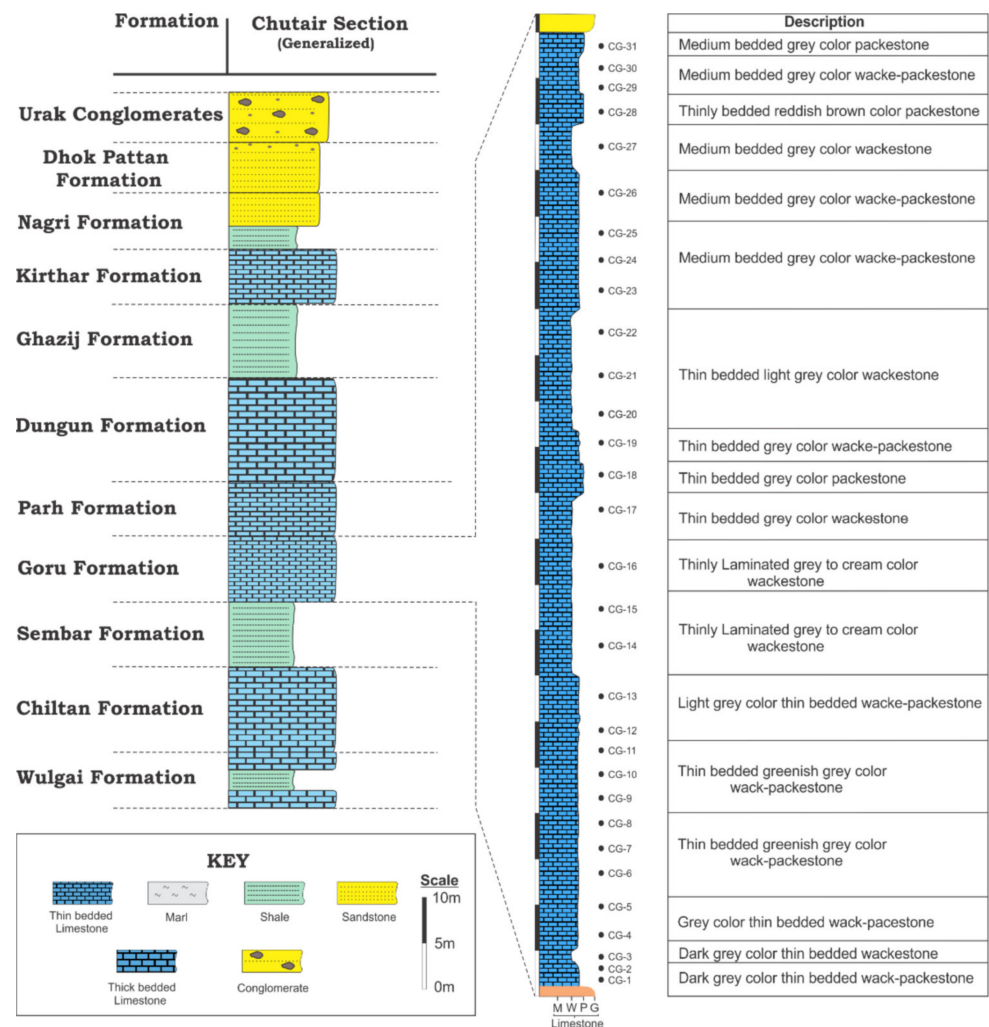


Figure 2. Generalized stratigraphy and lithologic log of Goru Formation at the study area, i.e., Chutair Section (After [3]).

3. Methodology

The Cretaceous pelagic carbonates of the Goru Formation exposed at Chutair Section (at Lat: 30°20'38.02" N; and Long: 67°54'11.26" E), Sulaiman Range is sampled for the determination of depositional environment, biostratigraphy, and sequence stratigraphy. The section is logged and 31 samples are collected on the basis of facies variation for the petrographic study [30]. The important features at the outcrop scale are noted. The field samples were cut into slabs and thin sections were generated at thin section laboratory of the National Centre of Excellence in Geology (NCE in Geology), University of Peshawar. The Nikon eclipse LV100ND polarizing microscope having dispersion staining observation at up to 400× magnification was used to examine and photograph the thin section at the Sedimentology and Paleontology Laboratory, NCE in Geology, University of Peshawar. The petrographic studies are carried out for the biostratigraphy and paleoenvironment. The morphological characteristics of planktonic foraminifera are used in association with published literature for identification [9,31,32]. For the sequence stratigraphic studies, the microfacies and biostratigraphy are used to define the system tracts and order of cycles, by using the sequence models from the literature [33,34].

4. Results and Discussions

4.1. Planktonic Foraminiferal Biostratigraphy

The planktonic foraminiferal studies are carried out for the determination of biostratigraphy of Goru Formation in the study area. Forty-four species of planktonic foraminifera that belonged to different genera are identified from thin section examination (Figure 3). Based on taxa's stratigraphic distribution within the Goru Formation in the study area (i.e., Chutair Section; Figure 1), 8 planktonic foraminiferal biozones are documented (Figure 4). These biozone are compared with literature [32,35–37]. The documented planktonic foraminifera are correlated with global biozonal schemes. All foraminiferal species' thin section photomicrographs are shown in Figure 3. The biozones discussed from the Albian–Turonian age of the pelagic carbonates of the Goru Formation are given as: *Muricohedbergella planispira* Interval Zone; *Ticinella primula* Interval Zone; *Biticinella breggiensis* Interval Zone; *Rotalipora appenninica* Interval Zone; *Rotalipora cushmani* Total Range Zone; *Whiteinella archeocretacea* Partial Range Zone; *Helvetoglobotruncana helvetica* Total Range Zone; and *Marginotruncana sigali* Partial Range Zone. These zones are discussed in detail as follows:

***Muricohedbergella Planispira* Interval Zone (Moullade, [38])**

Age: Early Albian

Definition: Partial range zone of *Muricohedbergella planispira* from the transition to the First Appearance Datum (FAD) of *Ticinella primula*.

Assemblage: *Muricohedbergella delrioensis*, *M. planispira* (Figures 3 and 4).

Remarks: This zone is marked based on the FAD of the *Ticinella primula*, and is characterized by the low-diversity assemblages. The zonal marker's FAD is recorded at the bottom of the section, and it may extend deeper into the unexposed stratigraphic depth, casting doubt on the Late Aptian age, although the base of the Albian is marked by the presence of *Microhedbergella renilaevis* [39] and in this part of the basin this particular species have not been identified (Figure 4).

***Ticinella Primula* Interval Zone (Moullade, [38])**

Age: Middle Albian

Definition: The zone ranges from the FAD of the *Ticinella primula* to the FAD of *Biticinella breggiensis*.

Assemblage: *Muricohedbergella delrioensis*, *M. planispira*, *M. rischi*, *M. simplex*, *Ticinella praeticinensis*, *T. primula*, *T. roberti* (Figures 3 and 4).

Remarks: The planktonic foraminifera gradually increase in this zone. Some of the planktonic species have their FADs in this zone including *M. rischi*, *M. simplex*, and *Ticinella roberti*. These taxa FADs have also been reported from this zone of the Parh Formation of Mughal Kot Section [40]. However, elsewhere in the world, the *Ticinella roberti* has been reported from the older Zone, i.e., *Ticinella bejaouaensis* zone [32,36]. This zone is correlated with the *Ticinella primula* zone of Premoli Silva and Verga [9].

***Biticinella Breggiensis* Interval Zone (Moullade, [38])**

Age: Middle Albian

Definition: This zone started from the FAD of *Biticinella breggiensis* to the FAD of *Rotalipora appenninica* and *Planomalina buxtorfi*.

Assemblage: *Biticinella breggiensis*, *B. subbreggiensis*, *Macroglobigerinelloides bentonensis*, *Muricohedbergella delrioensis*, *M. planispira*, *M. rischi*, *M. simplex*, *Ticinella praeticinensis*, *T. primula*, *T. raynaudi* (Figures 3 and 4).

Remarks: The upper boundary of this zone is marked on the FAD of *Rotalipora appenninica* and *Planomalina buxtorfi* instead of *Rotalipora ticinensis*, which is the defined boundary elsewhere in the world [32,38]. The diversity in the planktonic foraminifera increase in this zone such as *M. bentonensis*, *T. praeticinensis*, and *T. raynaudi*, start to appear in this zone.

***Rotalipora Appenninica* Interval Zone (Bronnimann, [41])**

Age: Late Albian

Definition: This interval spans from the FAD of *Rotalipora appenninica* to the FAD of *Rotalipora globotruncanoides*.

Assemblage: *Heterohelix moremani*, *H. reussi*, *Macroglobigerinelloides bentonensis*, *M. caseyi*, *Muricohedbergella delrioensis*, *M. planispira*, *M. rischi*, *M. simplex*, *Planomalina buxtorfi*, *P. praebuxtorfi*, *Praeglobotruncana delrioensis*, *Rotalipora appenninica*, *R. balernaensis*, *Ticinella madecassiana*, *T. primula* (Figures 3 and 4).

Remarks: The planktonic foraminiferal diversity and abundance increase. The keeled forms mostly appeared in this zone, i.e., *Rotalipora appenninica*, *Planomalina praebuxtorfi*, *P. buxtorfi*. The *Heterohelix moremani*, *H. reussi*, *Macroglobigerinelloides caseyi*, and *Praeglobotruncana delrioensis*, also appeared at the base of this zone (Figure 4). Some of the species disappeared in this zone, i.e., *Biticinella breggiensis*, *B. subbreggiensis*, *Ticinella primula*, *T. roberti*. The lower zones that were identified [9,32,36] are missing in this succession which with other factors could also be attributed to the coarse sampling in the field.

***Rotalipora Cushmani* Total Range Zone (Borsetti, [42])**

Age: Middle to Late Cenomanian

Definition: The Total range zone of *Rotalipora cushmani*.

Assemblage: *Heterohelix reussi*, *H. moremani*, *Muricohedbergella delrioensis*, *M. planispira*, *M. rischi*, *M. simplex*, *Macroglobigerinelloides bentonensis*, *Praeglobotruncana delrioensis*, *P. stephani*, *Rotalipora balernaensis*, *R. cushmani*, *R. globotruncanoides*, *R. greenhornensis*, *R. montsalvensis*, *Whiteinella baltica*, *W. praealvetica* (Figures 3 and 4).

Remarks: Most of the keeled taxa appeared in this zone. The test sizes showed increase towards the middle part and gradually started disappearing at the top. The *Whiteinella* and *Dicarinella* have their FADs in this zone (Figure 4). The *rotaliporids* are dominant in this zone and are reported in other parts of the world [9,32,42]. The *rotaliporids* are diversified and having the gradual disappearance of older species that is balanced by the younger species and then by *Whiteinella* and *Dicarinella* species. The *rotaliporids* have Last appearance datums (LADs) at the top of this zone that is also reported from elsewhere with the appearance of black shale, i.e., Ocean anoxic event-2 (OAE2) [14,36]. On the basis of bio-stratigraphic constraints, the black shale is correlated with the global bonarelli event (i.e., OAE2). Such black shales have also been reported from Parh Formation by Khan ([43]) from the Northern Suleman Range, Mughal Kot Section. However, in this study the black shale is not reported from this part of the basin in the southern Suleman Range. The planktonic foraminifera disappeared at the onset of these black shale deposition. Below this zone, some of the biozones are missing.

***Whiteinella Archeocretacea* Partial Range Zone (Bolli, [44])**

Age: Late Cenomanian to Early Turonian

Definition: This zone is the partial Range Zone of LAD of *Rotalipora cushmani* to the FAD of *Helvetoglobotruncana helvetica*.

Remarks: At the onset of black shale deposition, almost all the planktonic foraminifera disappeared. Consequently, this zone is only named based on the LAD of *Rotalipora cushmani* to the FAD of *Helvetoglobotruncana helvetica* as this zone is barren of foraminifera (Figure 4). The high organic rich black shale deposition corresponds to this zone [14,36]. Such black shales of OAE2 are not present in this part of the basin in the Goru Formation.

***Helvetoglobotruncana helvetica* Total Range Zone (Dalbiez, [45])**

Age: Early to middle Turonian

Definition: The total Range zone of *Helvetoglobotruncana helvetica*.

Assemblage: *Dicarinella algeriana*, *D. canaliculate*, *D. imbricata*, *Helvetoglobotruncana helvetica*, *Heterohelix moremani*, *H. reussi*, *Macroglobigerinelloides bentonensis*, *Muricohedbergella delrioensis*, *M. planispira*, *M. rischi*, *M. simplex*, *Marginotruncana coronata*, *M. marianosi*, *M. pseudolinneina*, *M. schneegansi*, *M. sigali*, *M. renzi*, *Praeglobotruncana gibba*, *P. stephani*, *W. aprica*, *W. baltica*, *W. brittonensis*, *W. paradubia*, and *Whiteinella praealvetica* (Figures 3 and 4).

Remarks: This zone started above the *Whiteinella archeocretacea* zone by the appearance of zonal marker that is FADs of *Helvetoglobotruncana helvetica* and extinction of *rotaliporids* (Figure 4). Some of the species survived this extinction like *Macroglobigerinelloides bentonensis*, and *Whiteinellids*. Most of the robust and large planktonic foraminifera have their FADs and diversification within this zone, i.e., *Marginotruncanids* like *Marginotruncana pseudolinneina*, *M. renzi*, *M. schneegansi*, and *M. sigali*.

Marginotruncana Sigali Partial Range Zone (Barr, [46])

Age: Late Turonian

Definition: This zone started from the extinction of *Helvetoglobotruncana helvetica*.

Assemblage: *Dicarinella canaliculate*, *D. concavata*, *D. imbricata*, *Heterohelix moremani*, *H. reussi*, *Muricohedbergella delrioensis*, *M. flandrini*, *M. planispira*, *M. rischi*, *M. simplex*, *Macroglobigerinelloides bentonensis*, *Marginotruncana coronata*, *M. pseudolinneina*, *M. mari-anosi*, *M. renzi*, *M. schneegansi*, *M. sigali*, and *M. undulata* (Figures 3 and 4).

Remarks: The base of this zone is marked by the LADs of *Praeglobotruncana* spp. and the extinction of *Helvetoglobotruncana helvetica* and FADs of *Muricohedbergella flandrini* and *Dicarinella concavata* (Figure 4). The upper boundary of this zone is not identified here. This zone is the last biozone that is encountered in the Goru Formation in the study area and is also observed elsewhere [32].

Biostratigraphic Discussions

The Goru Formation's planktonic foraminiferal biostratigraphy suggests Mid-Cretaceous (Early Albian to late Turonian) age in the study area (Figure 4). The planktonic foraminifera evolution in the mid-Cretaceous was defined by periods of high and low turnover. The latest Albian, the mid-Cenomanian, and the Cenomanian/Turonian boundary had the highest turnover rates [7]. All across the Cenomanian, the diversity remained high, with a wide range of morphologies [47]. The same type of conditions are also prevailing from vertebrate fauna of the peninsular India, and Cauvery Basin, India [48,49]. Almost all the identified zones in the Goru Formation are global in nature as was identified elsewhere [32,36]. The base of the deposition of pelagic carbonates of the Goru Formation started with *Muricohedbergella planispira* Zone that indicates the Early Albian age. This zone is marked based on the FAD of *Ticinella primula*. This is followed by the *Ticinella primula* Zone of Early Albian age in which the planktonic foraminifera become larger and abundant represented by the FAD of *Macroglobigerinelloides bentonensis* and *Muricohedbergella rischi*. In the same stage in Middle Albian time, the *Biticinella* appeared and have FAD in the *Biticinella breggiensis* Zone. Here, the notable increase in the taxa's diversity, and abundance and gradual transition in morphology from unkeeled to keeled taxa is observed. This zone is followed by the *Rotalipora appenninica* Zone of the latest Albian time in the study area. Some of the global biozone below *R. appenninica* Zone of the Late Albian are missing. Diversification of the *rotaliporids* occurs at the top of this zone where some species appeared. Some of the species become extinct at this zone that is *Ticinella's* and *biticinella's*. Above this zone, is the Total Range zone of *Rotalipora cushmani* Zone of Middle to Late Cenomanian age (Figure 4). Below this zone, some of the global biozone of Early Cenomanian age are missing in the Goru Formation that may be because of the coarse sampling intervals. At the top of this zone, is the zone OAE2 (Bonarelli event), but OAE2 black shale has not been identified in this part of the Suleman Range, despite the fact that the OAE2 black shale was identified in the Parh Formation of the Mughal Kot Section, northern Sulaiman Range [40]. This is correlated with the arbitrary biozone that is *Whiteinella archeocretacea* Biozone that is of the Latest Cenomanian to Early Turonian. Here, in the Goru Formation, the C/T (Cenomanian/Turonian) boundary is present in the pelagic carbonates. This arbitrary zone is marked on the LAD of *Rotalipora cushmani* to the FAD of *Helvetoglobotruncana helvetica*. With FAD of *Helvetoglobotruncana Helvetica*, the *Helvetoglobotruncana helvetica* Total Range Zone of the Early to Middle Turonian started where the large, robust *Marginotruncanids* appeared. After this, the *Marginotruncana sigali* Zone of Late Turonian age started with the extinction of the *Helvetoglobotruncana helvetica*. Here, the *Praeglobotruncana* disappear

and *Muricohedbergella flandrini* appeared. The Goru Formation deposition ends with this biozone in the Chutair Section, Sulaiman Range. The biozones identified in this study have been compared to the main Tethyan biozonation system on a global scale [9]. The Goru Formation's biostratigraphy also suggests that Cretaceous sedimentation in the Eastern Tethys was nearly complete.

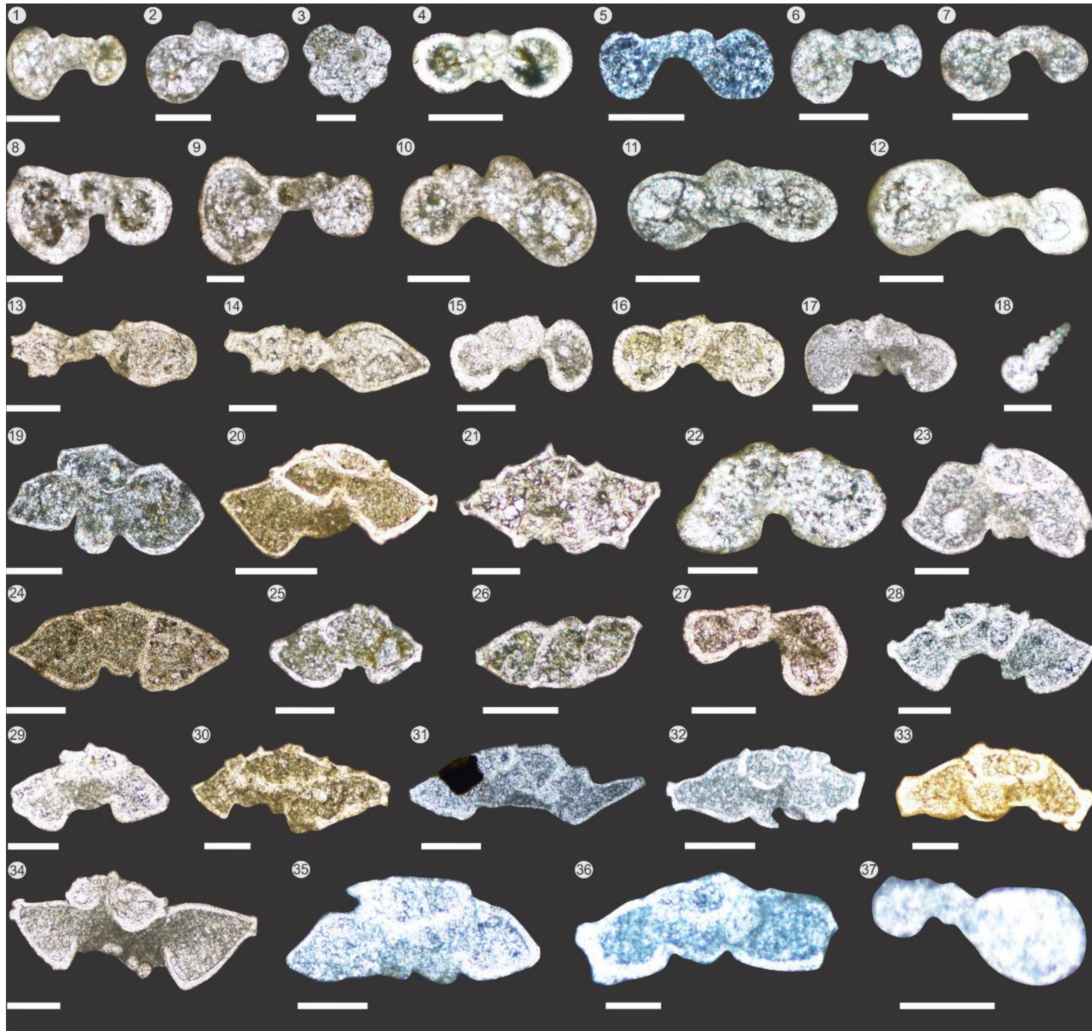


Figure 3. (1) *Muricohedbergella planispira*; (2) *Muricohedbergella delrioensis*; (3) *Ticinella primula*; (4) *Ticinella roberti*; (5) *Muricohedbergella simplex*; (6) *Muricohedbergella rischi*; (7) *Ticinella praeticinensis*; (8) *Biticnella subbreggiensis*; (9) *Biticnella breggiensis*; (10) *Ticinella madecassiana*; (11) *Ticinella raynaudi*; (12) *Macroglobigerinelloides bentonensis*; (13) *Planomalina praebuxtorfi*; (14) *Planomalina buxtorfi*; (15) *Whiteinella praehelvetica*; (16) *Whiteinella aprica*; (17) *Whiteinella brittonensis*; (18) *Heterohelix reussi*; (19) *Rotalipora cushmani*; (20) *Rotalipora globotruncanoids*; (21) *Rotalipora greenhornensis*; (22) *Praeglobotruncana delrioensis*; (23) *Praeglobotruncana gibba*; (24) *Rotalipora appenninica*; (25) *Rotalipora balernaensis*; (26) *Rotalipora montsalvensis*; (27) *Helvetoglobotruncana helvetica*; (28) *Marginotruncana sigali*; (29) *Marginotruncana Renzi*; (30) *Marginotruncana schneegansi*; (31) *Marginotruncana marianosi*; (32) *Marginotruncana coronata*; (33) *Marginotruncana pseudolinniena*; (34) *Dicarinella concavata*; (35) *Dicarinella imbricata*; (36) *Dicarinella canaliculata*; (37) *Muricohedbergella flandrini*. (Scale = 100 μ m).

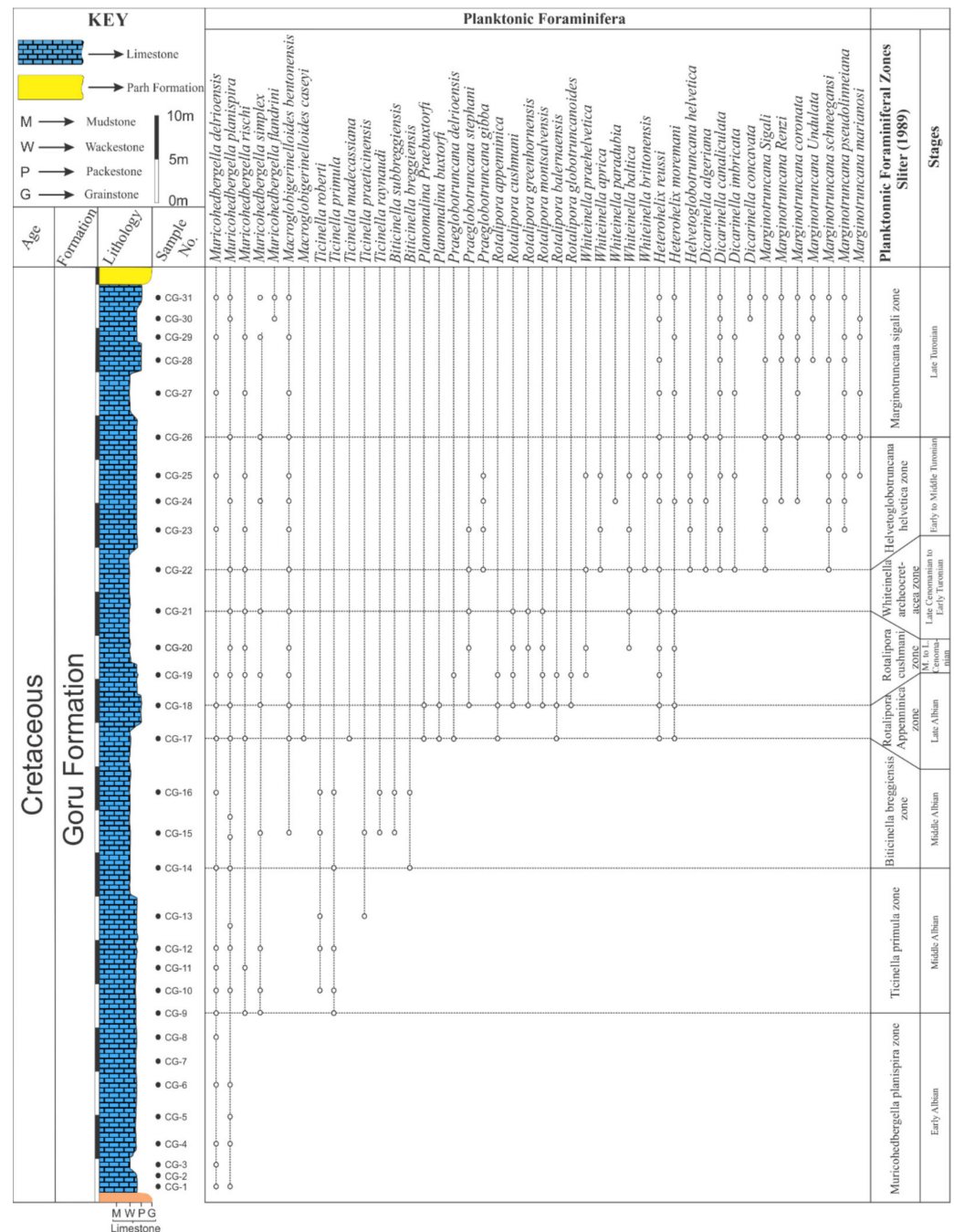


Figure 4. Biostratigraphic range chart of the Goru Formation exposed in the Chutair Section, Sulaiman Range.

4.2. Microfacies

The comprehensive petrographic analyses were carried out to evaluate the microfacies based depositional environment. Five microfacies were identified in the pelagic carbonates of the Goru Formation at Chutair Section based on texture, grain type, and other petrographic features discussed as follows:

4.2.1. Radiolarians-Rich Wacke-Packestone Microfacies (MF-1)

Description

The Radiolarians-rich wacke-packestone microfacies (MF-1) in the outcrop shows thin bedded dark grey color limestone. Petrographic observation reveals the presence

of matrix and allochems. The planktonic foraminifera, radiolarians, calcispheres, and undifferentiated bioclasts make up the majority of the allochems. The matrix is neomorphosed and ferruginous. (Figure 5).

Interpretation

The MF-1 microfacies is mostly comprised of the deeper fauna such as radiolarians and calcisphere. The radiolarians' dominance indicates that energy levels are too low and that they are found deeper in nature [50]. An environment with low-energy levels is reflected by the extensive carbonate mud. [50]. The combination of mud, radiolarians, and planktonic foraminifera indicate that the deposition took place in a low-energy environment [50,51]. The dominant radiolarians show deposition in the outer-ramp to deep basinal settings [52]. The MF-1 is deposited in deep basinal setting of the ramp depositional environment (Figure 6).

4.2.2. Radiolarians-Rich Wackestone Microfacies (MF-2)

Description

The Radiolarians-rich wackestone microfacies (MF-2) displays medium-bedded, dark grey to light grey limestone. The petrographic studies indicate the presence of grains and matrix. The radiolarian, calcisphere, and planktonic foraminiferal grains are present. The micrite is a fine bioclastic matrix that is ferruginous. (Figure 5).

Interpretation

The MF-2 has similar type of fauna to that of MF-1 but different texture. The radiolarians-rich deposit is found in deeper outer to basinal environments [53]. The presence of radiolarians and planktonic foraminifera together indicates a deeper energy condition. [54]. Hence, the MF-2 is deposited in the deeper basinal setting (Figure 6).

4.2.3. Planktonic Foraminiferal Wacke-Packestone Microfacies (MF-3)

Description

The Planktonic foraminiferal wacke-packestone microfacies (MF-3) shows thin to medium bedded grey to light grey color limestone. Planktonic foraminiferal allochems, mollusk bioclasts, and micritic matrix are the main components of this microfacies. The planktonic genera's includes the *Dicarinella*, *Macroglobigerinelloides*, *Marginotruncana*, *Muricohedbergella*, *Rotalipora*, *Ticinella* and *Whiteinella*. The other bioclasts include the mollusks, pelagic bivalves and some are undifferentiated. The radiolarians and calcisphere are in minor amount. This microfacies contains pyrite in the form of lenses and along the stylolites. The foraminiferal grains are concentrated at some places showing the tempestites nature (Figure 5).

Interpretation

The combined occurrences of the planktonic foraminifera, bioclasts of mollusks and radiolarians represents that the energy condition was low [50]. The concomitant of the radiolarians and planktonic foraminifera shows the deposition in outer ramp [54]. The pyrite rich matrix is present in most of the microfacies but here it is in more concentration, which is related to the OAEs of the cretaceous time [55,56]. Its presence represents the deeper water conditions. The tempestites in the microfacies represent the deposition near the stormy weather wave base (SWWB) [50]. The microfacies is deposited in proximal part of outer ramp setting (Figure 6).

4.2.4. Planktonic Foraminiferal Wackestone Microfacies (MF-4)

Description

The Planktonic foraminiferal wackestone microfacies (MF-4) in outcrop shows medium bedded grey limestone. The MF-4's major components are micritic matrix and allochems. Bioclasts are present and undifferentiated, while also belonging to bivalves, ostracodes, and echinoderms. The major planktonic foraminifera in MF-4 include *Dicarinella*, *Heterohelix*, *Macroglobigerinelloides*, *Marginotruncana*, *Muricohedbergella*, and *Whiteinella* (Figure 5).

Interpretation

There is a lot of lime mud in the MF-4. Lime mud's presence suggests low-energy conditions beneath the fair-weather wave base. [50]. The presence of bioclasts, as well as planktonic foraminifera and lime mud, support low-energy conditions [57]. Planktonic foraminifera show sediment deposition in an outer-ramp setting [30]. The microfacies suggest deposition in the proximal outer ramp environment (Figure 6).

4.2.5. Planktonic Foraminiferal Packestone Microfacies (MF-5)

Description

The Planktonic foraminiferal packestone microfacies (MF-5) is identified by the presence of a micritic matrix, foraminiferal grains, and pyrite. The micritic matrix is fine bioclastic matrix. *Dicarinella*, *Heterohelix*, *Marginotruncana*, and *Muricohedbergella*, and *Whiteinella* are the dominant foraminifera present in MF-5. The foraminiferal chambers are filled with pyrite. The micritic matrix contains a significant amount of brown pyrite. The pyritization also occurred along the stylolites. Additionally, there are radiolarians, a small number of calcispheres, and sponge spicules. (Figure 5).

Interpretation

The pyrite is in the form of matrix and suture boundaries is the dominant feature of this microfacies. The lack of neritic fauna and dominance of the pyritic matrix shows deposition in outer ramp setting [43]. The coexistence of radiolarians and planktonic foraminifera supports deposition in outer ramp environments [54]. In the light of the above-mentioned biota and other features, distal outer ramp environment is suggested for this microfacies (Figure 6).

4.2.6. Depositional Environment

The geoscientists need to understand the depositional environment since it determines the architecture, heterogeneity, and ultimately the quality of any reservoirs [58–61]. The Goru Formation is the study area and is comprised of pelagic thin bedded carbonates. Based on petrographic studies, the texture is wackestone, wacke-packestone, and packestone. Allochems and micritic matrix are the most important constituents. The grains are of radiolarians, calcispheres, planktonic foraminifera, whilst others are bioclasts. The majority of the bioclasts are undifferentiated, although some are planktonic foraminifera and mollusks (bivalves), ostracodes and echinoderms. The micritic matrix is fine and mud dominated. The limestone's mud-dominated texture indicates that the mud was deposited from a suspended load in a low-energy environment [62]. A deep marine outer ramp energy setting below the storm wave base is suggested by the presence of planktonic foraminifera in the limestone unit [30]. The other grains such as radiolarians and calcisphere indicate the deeper water conditions [54]. Radiolarians are a key paleoenvironmental indicator that accumulate on the seabed because of suspended load, but they may also be found in the outer ramp setting [63]. The high content of radiolarians, planktonic foraminifera together with pelagic lime mud show outer ramp setting. Based on the microfacies details, the sediments of the Goru Formation are pelagic in nature and were deposited in the distal middle ramp via distal outer ramp to deep basal setting in low-energy conditions (Figure 6). The ramp depositional environment was suggested for these carbonates because there is nothing about the deposition of resedimented deposits, i.e., turbidities, and also there is nothing about the grain stone belts and reefal offshore facies. All this evidence suggests a low-energy gradient slope that is the feature of ramp rather than a shelf [64].

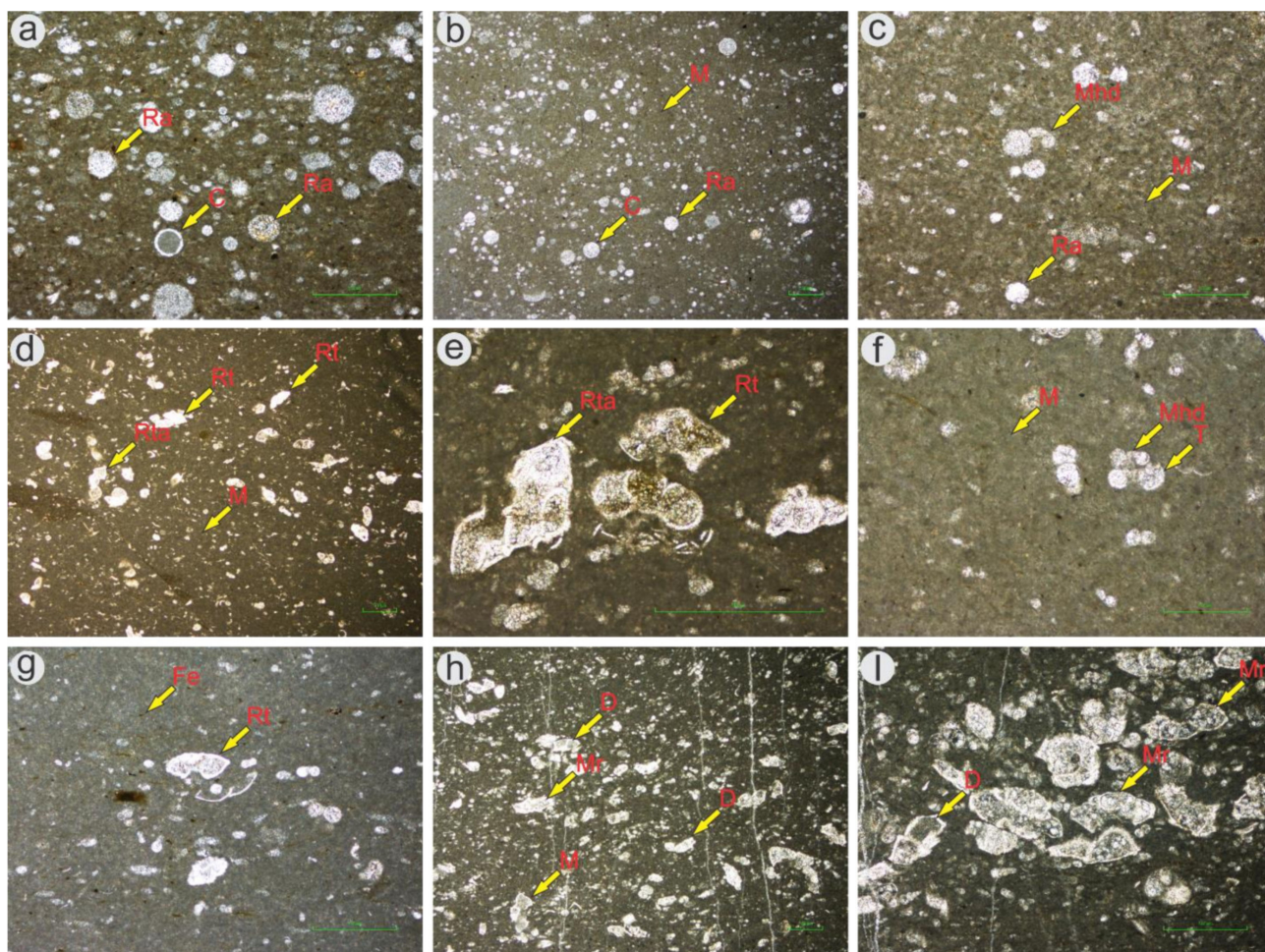


Figure 5. (a) Photomicrograph of the Radiolarians rich wacke-packestone microfacies (MF-1) showing radiolarians (Ra) and Calcisphere (C); (b) Photomicrograph of the MF-1 (zoomed view) showing matrix (M), radiolarians (Ra) and Calcisphere (C); (c) Photomicrograph of the Radiolarians rich wackestone microfacies (MF-2) showing radiolarians (Ra), matrix (M) and *muricohedbergella* (Mhd); (d) Photomicrograph of the Planktonic foraminiferal wacke-packestone microfacies (MF-3) showing *rotalipora* sp. (Rt), *rotalipora appenninica* (Rta), and matrix (M); (e) Photomicrograph of the MF-3 (zoomed view) showing *Rotalipora appenninica* (Rta), and *rotalipora* sp. (Rt); (f) Photomicrograph of the Planktonic foraminiferal wackestone microfacies (MF-4) having *muricohedbergella* (Mhd), *Ticinella* (T) and matrix (M); (g) Photomicrograph of the MF-4 (zoomed view) having iron filaments (Fe) and *rotalipora* (Rt); (h) Photomicrograph of the Planktonic Foraminiferal Packestone Microfacies (MF-5) showing *marginotruncana* (M) and *dicarinella* (D); (i) Photomicrograph of the MF-5 (zoomed view) having *dicarinella* (D); and *marginotruncana* (M).

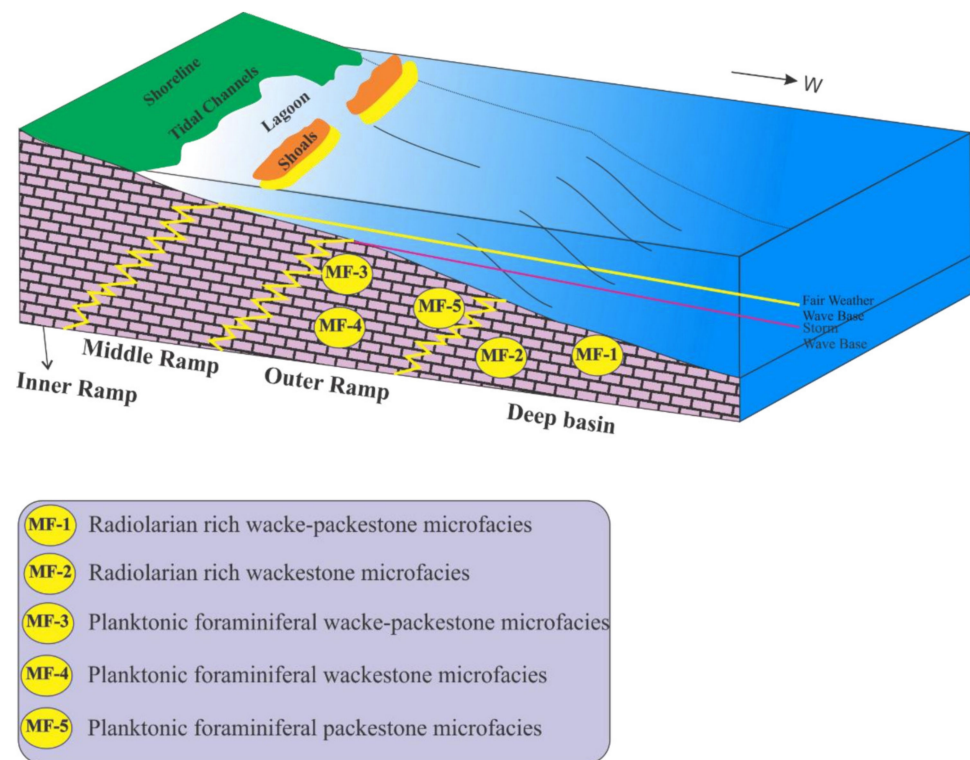


Figure 6. Proposed depositional model of the Goru Formation at Chutair Section, Sulaiman Range.

4.3. Sequence Stratigraphy

The microfacies studies along with bio-stratigraphic investigations of the pelagic carbonates of the Goru Formation are done, which indicates the outer ramp to deep basinal environment of deposition for the pelagic carbonates of Goru Formation in Albian to Turonian time (Figure 4). It is essential to classify depositional sequences according to their cyclicity orders because tectonics controls the eustatic rise and fall that might occur throughout a series of time periods [65]. Each sequence is the result of a specific tectonic or eustatic cycle order. The stratigraphic cycle is usually demonstrated in the following four orders of million years' time span [66]. That is, the first order (greater than 50 Ma), second order (3–50 Ma), third order (0.5–3 Ma), and fourth order (0.1–0.5 Ma) order of cycles [65,67]. The current bio-stratigraphic results show an Albian to Turonian age (113–89.8 Ma) for the deposition of Goru Formation in the study area (Figure 3). This represents an overall time span of 23.2 Ma for the deposition of Goru Formation. This time indicates that the Goru Formation is deposited in Second (2nd) order cycle. For the third (3rd) order cyclicity, the Transgressive-Regressive (T-R) sequence model [33] is used. The T-R sequence model employs the unconformable portion of the boundary as sub-aerial unconformity over the basin margin, and the correlative conformity as the maximum regressive surface (MRS) farther seaward. This model provides a special technique of classifying strata into sequences. T-R sequences are classified as transgressive systems tract (TST) or regressive systems tract (RST) based on Maximum Flooding Surfaces (MFS) (Figure 7). Six depositional sequences are identified that represent system tracts [68,69]. Two types of system tracts that is TST and RST are identified by using the T-R sequence model in a measured section of the Goru Formation in the Chutair Section.

4.3.1. Depositional Sequences

Depending on the sequence model used, depositional sequence corresponds to the depositional product of a whole cycle of base-level changes or shoreline movements [68]. The consequence of the interactions between Eustasy, climate, and tectonic, the depositional

sequence constitutes a full cycle of deposition [65,70]. In the Goru Formation, the identified sequences contain total of eleven system tracts, which are the following.

4.3.2. System Tracts

Transgressive system tract (TST)

Six transgressive system tracts are identified comprising of the deeper pelagic carbonates of the Goru Formation. All the transgressive system tracts (TST1-TST6) represent a retro gradational stacking pattern that is the shallower microfacies are overlain by deeper microfacies (Figure 7). The TST1 and TST2 contains the deep basinal microfacies that are overlain by the proximal outer ramp microfacies. The TST3-TST5 are represented by the distal outer ramp microfacies that are overlain by the proximal outer ramp microfacies. The TST6 shows distal outer microfacies that is present at the top of the Formation and also overlain by the proximal outer ramp microfacies. Stratigraphically, the TST1, TST2, and TST3 are present in the Albian time. The TST4 in late Cenomanian to Early Turonian and TST5, TST6 in the Late Turonian time (Figure 7).

Regressive System tract (RST)

Five regressive system tracts are identified comprising of outer ramp carbonates of the Goru Formation. The regressive system tracts are characterized by the progradational facies pattern that is the deeper facies are overlain by the shallower facies (Figure 7). The RST1 is represented by the proximal outer ramp microfacies that is underlain and overlain by of deep basinal microfacies. The RST2 contains the same microfacies as that of RST1 that is the proximal outer ramp microfacies. The RST2 is underlain by deeper basinal microfacies and overlain by the distal outer ramp microfacies. The RST3, RST4, and RST5 is represented by proximal outer ramp microfacies and overlain by distal outer ramp microfacies. Similarly, the bio stratigraphic position of the RST1, and RST2 are present in Albian time. The RST3 in late Cenomanian to Early Turonian time and RST4, RST5 in Middle to Late Turonian time (Figure 7).

4.3.3. Comparison of Local with Global Sea Level Curve

The Cretaceous is defined by the long- and short-term sea level oscillations [71]. The overall trend of sea level in the Cretaceous is characterized by a fall in the Cenomanian, a maximum rise in the early Turonian, a prolonged fall from the middle Turonian to the Santonian, a rise in the late Santonian to the early Campanian, and then a subsequent fall in the Middle Campanian that lasts until the Danian [72]. Long-term sea-level variations can be connected to paleoclimate, for example, the boundary between the late Cenomanian and early Turonian is documented as a worldwide warming event of OAE2 defined by positive $\delta^{13}\text{C}$ excursion, high organic burial and global sea level rise [4,56,73]. The Cretaceous' maximum sea-level increase occurred during the Earliest Turonian (93.5), and is believed to have been 240–250 m. above present-day mean sea level (or 180–190 m without the existing ice cap, which is anticipated to store water equal to another 60 m of sea-level rise) [71]. Therefore, the sea level curve of the Goru Formation is constructed on the basis of microfacies types under the bio stratigraphic framework. This local sea level curve of the formation is compared with the global curve of Haq et al., [34] to infer about the global and local tectonic on the Goru Formation deposition. The Long-term sea-level variations in Goru Formation have continued to deposit a second-order composite transgressive systems tract, which is comparable with Haq et al.'s, [34] long-term sea-level curve (Figure 7). The short-term 3rd order sea level fluctuations show six episodes of rise and fall, whilst the Haq et al., [34] curve shows almost double to these conditions (Figure 7). The difference in the short-term pattern of sea-level variation in the study area from the global short-term sea-level curve at the time of deposition is attributed to the local tectonics in the study area.

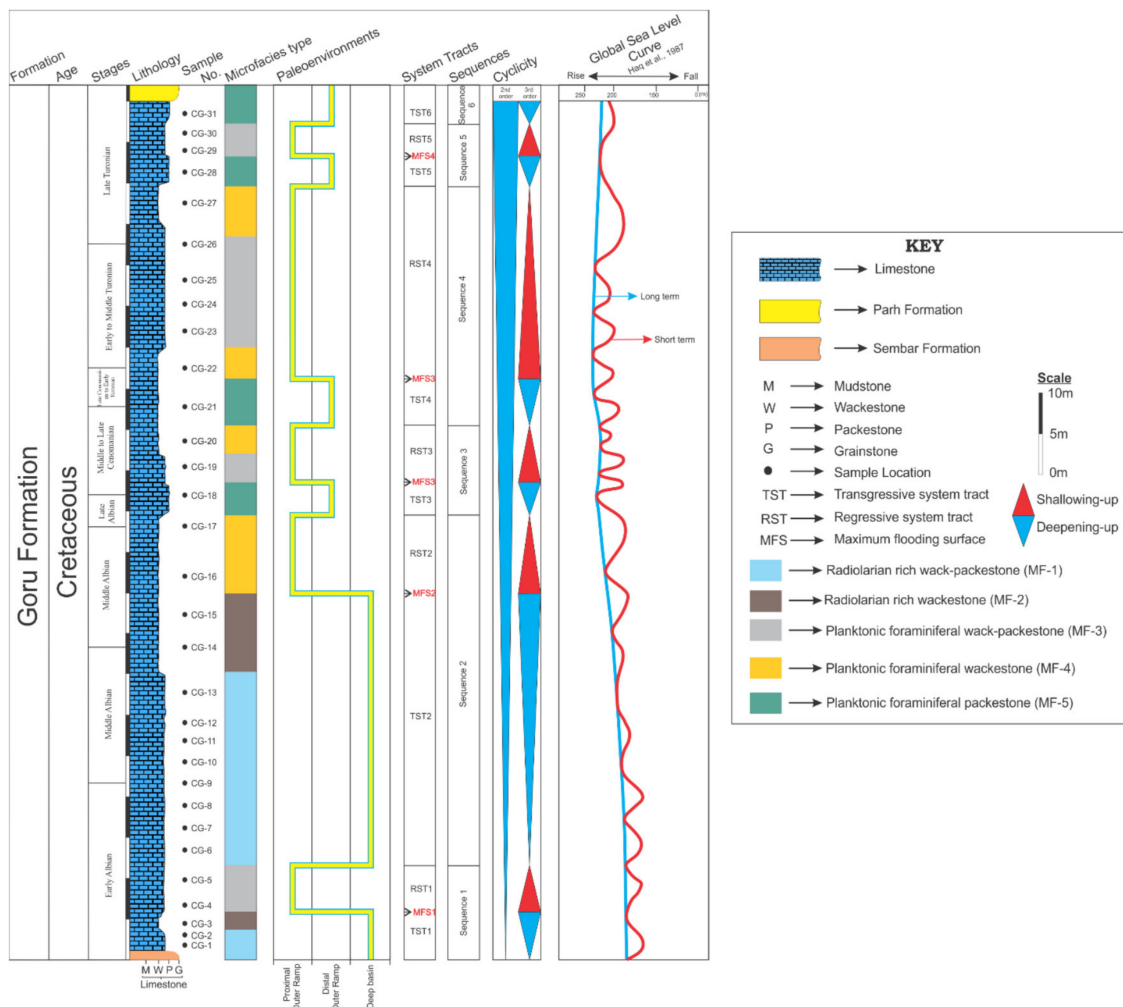


Figure 7. Showing the vertical distribution of microfacies, paleoenvironment, vertical distribution of sequences and system tracts, global sea level curve of the Goru Formation at Chutair Section, Sulaiman Range, Pakistan.

5. Conclusions

The Cretaceous Goru Formation in the study area is comprised of thin to medium bedded, greenish grey, whitish and dark grey color pelagic carbonates. Based on planktonic foraminiferal biostratigraphic studies, eight biozones are established: *Muricohedbergella planispira* Interval Zone; *Ticinella primula* Interval Zone; *Biticinella breggiensis* Interval Zone; *Rotalipora appenninica* Interval Zone; *Rotalipora cushmani* Total Range Zone; *Whiteinella archeocretacea* Partial Range Zone; *Helvetoglobotruncana helvetica* Total Range Zone; and *Marginotruncana sigali* Partial Range Zone. Based on these biozones, an Albian–Turonian (113–89.8 Ma) age is assigned to the Goru Formation in the study area. The detailed petrographic studies revealed five microfacies types, namely: radiolarians rich wack-packestone (deep basinal settings); radiolarians rich wackestone (deep basinal settings); planktonic foraminiferal wack-packestone; planktonic foraminiferal wackestone; and planktonic foraminiferal packestone suggesting deposition of Goru Formation in outer ramp to deep basinal settings. The biostratigraphic and microfacies types are used to establish sequence stratigraphic studies that show transgressive and regressive sea level episodes in the Goru Formation. Six depositional sequences are established that include eleven system tracts including six transgressive and five regressive system tracts ranging from Albian to Turonian age. Two orders of cycles are identified including 2nd and 3rd order. The overall deposition of the Goru Formation takes place at 2nd order of cycle which includes

the small-scale 3rd order cycles. The 2nd order local sea level curve of the Goru Formation is matching with the Global Sea level curve whilst the 3rd order curve is not that much matching showing a local tectonic control in the difference in the 3rd order cyclicity.

Author Contributions: S.U., I.U.J. and M.H. proposed the main concept and involved in write up. K.L. and M.M. helped in collection of field data. M.S. and A.A. helped in lab work, preparation of figures and establishing biostratigraphy. U.A. and H.V.T. did provision of relevant literature, review and proofread of the manuscript. All authors have read and agreed to the published version of the manuscript.

Funding: This research work was funded by National Centre of Excellence in Geology, University of Peshawar and PSF-TUBITAK project having project no. PSF-TUBITAK/Earth/KP-UoP (08) by the Pakistan Science Foundation.

Data Availability Statement: Not applicable.

Acknowledgments: The research provided in this paper was conducted as part of the first author's doctoral dissertation. Authors are thankful to the National Centre of Excellence in Geology, University of Peshawar for providing funds for field work. Thanks are extended to Mukhtiar Ghani, Geological Survey Pakistan, for his help during geological field work. The authors acknowledge the PSF-TUBITAK project having project no. PSF-TUBITAK/Earth/KP-UoP (08), which was given to Muhammad Hanif at the National Centre of Excellence in Geology, University of Peshawar by the Pakistan Science Foundation for providing funds for the laboratory analysis.

Conflicts of Interest: The authors declare no conflict of interest.

References

1. Afzal, J.; Williams, M.; Aldridge, R.J. Revised stratigraphy of the lower Cenozoic succession of the Greater Indus Basin in Pakistan. *J. Micropalaeontol.* **2009**, *28*, 7–23. [[CrossRef](#)]
2. Kassi, A.M.; Kelling, G.; Kasi, A.K.; Umar, M.; Khan, A.S. Contrasting Late Cretaceous–Palaeocene lithostratigraphic successions across the Bibai Thrust, western Sulaiman Fold–Thrust Belt, Pakistan: Their significance in deciphering the early-collisional history of the NW Indian Plate margin. *J. Asian Earth Sci.* **2009**, *35*, 435–444. [[CrossRef](#)]
3. Shah, S. Stratigraphy of Pakistan (memoirs of the geological survey of Pakistan). *Geol. Surv. Pak.* **2009**, *22*, 381.
4. Jenkyns, H. Cretaceous anoxic events: From continents to oceans. *J. Geol. Soc.* **1980**, *137*, 171–188. [[CrossRef](#)]
5. Weissert, H.; Erba, E. Volcanism, CO₂ and palaeoclimate: A Late Jurassic–Early Cretaceous carbon and oxygen isotope record. *J. Geol. Soc.* **2004**, *161*, 695–702. [[CrossRef](#)]
6. Jones, C.E.; Jenkyns, H.C. Seawater strontium isotopes, oceanic anoxic events, and seafloor hydrothermal activity in the Jurassic and Cretaceous. *Am. J. Sci.* **2001**, *301*, 112–149. [[CrossRef](#)]
7. Leckie, R.M.; Bralower, T.J.; Cashman, R. Oceanic anoxic events and plankton evolution: Biotic response to tectonic forcing during the mid-Cretaceous. *Paleoceanography* **2002**, *17*, 13–1–13–29. [[CrossRef](#)]
8. Wang, T.; Li, G.; Aitchison, J.C.; Ding, L.; Sheng, J. Evolution of mid-Cretaceous radiolarians in response to oceanic anoxic events in the eastern Tethys (southern Tibet, China). *Palaeogeogr. Palaeoclimatol. Palaeoecol.* **2019**, *536*, 109369. [[CrossRef](#)]
9. Premoli Silva, I.; Verga, D. *Practical Manual of Cretaceous Planktonic Foraminifera*; Tipografia Pontefelcino: Perugia, Italy, 2004; p. 283.
10. Leckie, R.M. A paleoceanographic model for the early evolutionary history of planktonic foraminifera. *Palaeogeogr. Palaeoclimatol. Palaeoecol.* **1989**, *73*, 107–138. [[CrossRef](#)]
11. Poulsen, C.J.; Barron, E.J.; Arthur, M.A.; Peterson, W.H. Response of the mid-Cretaceous global oceanic circulation to tectonic and CO₂ forcings. *Paleoceanography* **2001**, *16*, 576–592. [[CrossRef](#)]
12. Erbacher, J.; Thurow, J. Influence of oceanic anoxic events on the evolution of mid-Cretaceous radiolaria in the North Atlantic and western Tethys. *Mar. Micropaleontol.* **1997**, *30*, 139–158. [[CrossRef](#)]
13. Hart, M.B. The evolution and biodiversity of Cretaceous planktonic Foraminifera. *Geobios* **1999**, *32*, 247–255. [[CrossRef](#)]
14. Premoli Silva, I.; Sliter, W. Cretaceous planktonic foraminiferal biostratigraphy and evolutionary trends from the Bottaccione section, Gubbio, Italy. *Palaeontogr. Ital.* **1994**, *82*, 1–89.
15. Shafique, N.A.; Daniels, C. Foraminiferal zonation of Upper Goru Formation–Bawani area, Kirthar Range. *Pak. J. Hydrocarb. Res.* **1990**, *2*, 67–84.
16. Ashraf, U.; Zhang, H.; Anees, A.; Nasir Mangi, H.; Ali, M.; Ullah, Z.; Zhang, X. Application of unconventional seismic attributes and unsupervised machine learning for the identification of fault and fracture network. *Appl. Sci.* **2020**, *10*, 3864. [[CrossRef](#)]
17. Ashraf, U.; Zhu, P.; Yasin, Q.; Anees, A.; Imraz, M.; Mangi, H.N.; Shakeel, S. Classification of reservoir facies using well log and 3D seismic attributes for prospect evaluation and field development: A case study of Sawan gas field, Pakistan. *J. Pet. Sci. Eng.* **2019**, *175*, 338–351. [[CrossRef](#)]

18. Ashraf, U.; Zhang, H.; Anees, A.; Ali, M.; Zhang, X.; Shakeel Abbasi, S.; Nasir Mangi, H. Controls on reservoir heterogeneity of a shallow-marine reservoir in Sawan Gas Field, SE Pakistan: Implications for reservoir quality prediction using acoustic impedance inversion. *Water* **2020**, *12*, 2972. [[CrossRef](#)]
19. Ashraf, U.; Zhang, H.; Anees, A.; Mangi, H.N.; Ali, M.; Zhang, X.; Imraz, M.; Abbasi, S.S.; Abbas, A.; Ullah, Z. A core logging, machine learning and geostatistical modeling interactive approach for subsurface imaging of lenticular geobodies in a clastic depositional system, SE Pakistan. *Nat. Resour. Res.* **2021**, *30*, 2807–2830. [[CrossRef](#)]
20. Dar, Q.U.; Pu, R.; Baiyegunhi, C.; Shabeer, G.; Ali, R.I.; Ashraf, U.; Sajid, Z.; Mehmood, M. The impact of diagenesis on the reservoir quality of the early Cretaceous Lower Goru sandstones in the Lower Indus Basin, Pakistan. *J. Pet. Explor. Prod. Technol.* **2022**, *12*, 1437–1452. [[CrossRef](#)]
21. Kazmi, A.H.; Abbasi, I.A. *Stratigraphy & Historical Geology of Pakistan*; Department & National Centre of Excellence in Geology: Peshawar, Pakistan, 2008.
22. Williams, M.D. Stratigraphy of the Lower Indus Basin, West Pakistan. In Proceedings of the 5th World Petroleum Congress, New York, NY, USA, 1–5 June 1959.
23. Shafique, N.A. *Spatial Biostratigraphy of NW Pakistan*; Miami University: Oxford, OH, USA, 2001.
24. Smewing, J.D.; Warburton, J.; Daley, T.; Copestake, P.; Ul-Haq, N. Sequence stratigraphy of the southern Kirthar fold belt and middle Indus basin, Pakistan. *Geol. Soc. Lond. Spec. Publ.* **2002**, *195*, 273–299. [[CrossRef](#)]
25. Haq, S.S.; Davis, D.M. Oblique convergence and the lobate mountain belts of western Pakistan. *Geology* **1997**, *25*, 23–26. [[CrossRef](#)]
26. Jadoon, I.A.; Lawrence, R.D.; Lillie, R.J. Seismic data, geometry, evolution, and shortening in the active Sulaiman fold-and-thrust belt of Pakistan, southwest of the Himalayas. *AAPG Bull.* **1994**, *78*, 758–774.
27. Lawrence, R.; Yeats, R.; Khan, S.; Farah, A.; DeJong, K. Thrust and strike slip fault interaction along the Chaman transform zone, Pakistan. *Geol. Soc. Lond. Spec. Publ.* **1981**, *9*, 363–370. [[CrossRef](#)]
28. Riaz, M.S.; Bin, S.; Naeem, S.; Kai, W.; Xie, Z.; Gilani, S.M.M.; Ashraf, U. Over 100 years of faults interaction, stress accumulation, and creeping implications, on Chaman Fault System, Pakistan. *Int. J. Earth Sci.* **2019**, *108*, 1351–1359. [[CrossRef](#)]
29. Raza, S.M.; Cheema, I.U.; Downs, W.R.; Rajpar, A.R.; Ward, S.C. Miocene stratigraphy and mammal fauna from the Sulaiman Range, Southwestern Himalayas, Pakistan. *Palaeogeogr. Palaeoclimatol. Palaeoecol.* **2002**, *186*, 185–197. [[CrossRef](#)]
30. Flügel, E. *Microfacies of Carbonate Rocks: Analysis, Interpretation and Application*; Springer: Berlin/Heidelberg, Germany, 2013.
31. Postuma, J.A. *Manual of Planktonic Foraminifera*; Elsevier: Amsterdam, The Netherlands, 1971.
32. Sliter, W.V. Biostratigraphic zonation for Cretaceous planktonic foraminifers examined in thin section. *J. Foraminif. Res.* **1989**, *19*, 1–19. [[CrossRef](#)]
33. Embry, A.; Johannessen, E. T-R sequence stratigraphy, facies analysis and reservoir distribution in the uppermost Triassic–Lower Jurassic succession, western Sverdrup Basin, Arctic Canada. In *Norwegian Petroleum Society Special Publications*; Elsevier: Amsterdam, The Netherlands, 1993; Volume 2, pp. 121–146.
34. Haq, B.U.; Hardenbol, J.; Vail, P.R. Chronology of fluctuating sea levels since the Triassic. *Science* **1987**, *235*, 1156–1167. [[CrossRef](#)] [[PubMed](#)]
35. Amédro, F.; Matrimon, B.; Magniez-Jannin, F.; Touch, R. La limite Albien inférieur-Albien moyen dans l’Albien type de l’Aube (France): Ammonites, foraminifères, séquences. *Rev. Paléobiol.* **2014**, *33*, 159–279.
36. Caron, M.; Bolli, H.; Saunders, J.; Perch-Nielsen, K. Cretaceous planktic foraminifera. *Plankton Stratigr.* **1985**, *1*, 17–86.
37. Petrizzo, M.R.; Gilardoni, S.E. Planktonic foraminiferal biostratigraphy of late Albian-Cenomanian pelagic sequences from the Umbria-Marche basin (central Italy) and the Mazagan Plateau (northeast Atlantic Ocean). *Riv. Ital. Paleontol. E Stratigr.* **2020**, *126*, 865–904.
38. Moullade, M. *Étude Stratigraphique et Micropaléontologique du Crétacé Inférieur de La “Fosse Vocontienne”*; Université de Lyon: Lyon, France, 1966; Volume 15.
39. Kennedy, J.W.; Gale, A.S.; Huber, B.T.; Petrizzo, M.R.; Bown, P.; Jenkyns, H.C. The Global Boundary Stratotype Section and Point (GSSP) for the base of the Albian Stage, of the Cretaceous, the Col de Pré-Guittard section, Arnanon, Drôme, France. *Epis. J. Int. Geosci.* **2017**, *40*, 177–188. [[CrossRef](#)]
40. Khan, S.; Kroon, D.; Wadood, B.; Ahmad, S.; Zhou, X. Marine depositional signatures of the Aptian Oceanic Anoxic Events in the Eastern Tethys, Lower Indus Basin, Pakistan. *Aust. J. Earth Sci.* **2022**, *69*, 251–267. [[CrossRef](#)]
41. Brönnimann, P. *Globigerinidae from the Upper Cretaceous (Cenomanian-Maestrichtian of Trinidad, BWI)*; Paleontological Research Institution: Ithaca, NY, USA, 1952.
42. Borsetti, A. Foraminiferi planctonici di una serie cretacea dei Dintorni di Piobbico (Prov. di Pesaro). *G. Geol. Ser.* **1962**, *2*, 19–75.
43. Khan, S.; Kroon, D.; Ahmad, S.; Ali, A.; Wadood, B.; Rahman, A. Planktonic foraminiferal biostratigraphy of the Cretaceous strata, Indus Basin, Pakistan, Eastern Tethys: Implications for oceanic anoxic events. *Aust. J. Earth Sci.* **2021**, *68*, 1162–1178. [[CrossRef](#)]
44. Bolli, H.M. *Zonation of Cretaceous to Pliocene Marine Sediments Based on Planktonic Foraminifera*; Geologisches Institut der Eidg. Technischen Hochschule und der Universität Zürich: Zürich, Switzerland, 1966.
45. Dalbiez, F. The genus Globotruncana in Tunisia. *Micropaleontology* **1955**, *1*, 161–171. [[CrossRef](#)]
46. Barr, F. Cretaceous biostratigraphy and planktonic foraminifera of Libya. *Micropaleontology* **1972**, *18*, 1–46. [[CrossRef](#)]
47. Friedrich, O.; Norris, R.D.; Erbacher, J. Evolution of middle to Late Cretaceous oceans—A 55 my record of Earth’s temperature and carbon cycle. *Geology* **2012**, *40*, 107–110. [[CrossRef](#)]

48. Khosla, A.; Verma, O. Paleobiota from the Deccan volcano-sedimentary sequences of India: Paleoenvironments, age and paleobiogeographic implications. *Hist. Biol.* **2015**, *27*, 898–914. [[CrossRef](#)]
49. Verma, O. Cretaceous vertebrate fauna of the Cauvery Basin, southern India: Palaeodiversity and palaeobiogeographic implications. *Palaeogeogr. Palaeoclimatol. Palaeoecol.* **2015**, *431*, 53–67. [[CrossRef](#)]
50. Flügel, E.; Munnecke, A. *Microfacies of Carbonate Rocks: Analysis, Interpretation and Application*; Springer: Berlin/Heidelberg, Germany, 2010; Volume 976.
51. Ghabeishavi, A.; Vaziri-Moghaddam, H.; Taheri, A.; Taati, F. Microfacies and depositional environment of the Cenomanian of the Bangestan anticline, SW Iran. *J. Asian Earth Sci.* **2010**, *37*, 275–285. [[CrossRef](#)]
52. Gawlick, H.-J.; Schlagintweit, F. Berriasian drowning of the Plassen carbonate platform at the type-locality and its bearing on the early Eoalpine orogenic dynamics in the Northern Calcareous Alps (Austria). *Int. J. Earth Sci.* **2006**, *95*, 451–462. [[CrossRef](#)]
53. Haas, J.; Götz, A.E.; Pálfy, J. Late Triassic to Early Jurassic palaeogeography and eustatic history in the NW Tethyan realm: New insights from sedimentary and organic facies of the Csóvár Basin (Hungary). *Palaeogeogr. Palaeoclimatol. Palaeoecol.* **2010**, *291*, 456–468. [[CrossRef](#)]
54. Heldt, M.; Bachmann, M.; Lehmann, J. Microfacies, biostratigraphy, and geochemistry of the hemipelagic Barremian–Aptian in north-central Tunisia: Influence of the OAE 1a on the southern Tethys margin. *Palaeogeogr. Palaeoclimatol. Palaeoecol.* **2008**, *261*, 246–260. [[CrossRef](#)]
55. Jenkyns, H.; Gale, A.; Corfield, R. Carbon and oxygen isotope stratigraphy of the English Chalk and Italian Scaglia and its palaeoclimatic significance. *Geol. Mag.* **1994**, *131*, 1–34. [[CrossRef](#)]
56. Takashima, R.; Nishi, H.; Huber, B.T.; Leckie, R.M. Greenhouse world and the Mesozoic ocean. *Oceanography* **2006**, *19*, 82–92. [[CrossRef](#)]
57. Wilson, J. *Carbonate Facies in Geologic History*; Springer: New York, NY, USA, 1975; p. 471.
58. Anees, A.; Zhang, H.; Ashraf, U.; Wang, R.; Liu, K.; Abbas, A.; Ullah, Z.; Zhang, X.; Duan, L.; Liu, F. Sedimentary facies controls for reservoir quality prediction of lower shihezi member-1 of the Hangjinqi area, Ordos Basin. *Minerals* **2022**, *12*, 126. [[CrossRef](#)]
59. Anees, A.; Zhang, H.; Ashraf, U.; Wang, R.; Liu, K.; Mangi, H.; Jiang, R.; Zhang, X.; Liu, Q.; Tan, S. Identification of Favorable Zones of Gas Accumulation Via Fault Distribution and Sedimentary Facies: Insights from Hangjinqi Area, Northern Ordos Basin. *Front. Earth Sci.* **2022**, *9*, 822670. [[CrossRef](#)]
60. Thanh, H.V.; Sugai, Y. Integrated modelling framework for enhancement history matching in fluvial channel sandstone reservoirs. *Upstream Oil Gas Technol.* **2021**, *6*, 100027. [[CrossRef](#)]
61. Vo Thanh, H.; Lee, K.-K. 3D geo-cellular modeling for Oligocene reservoirs: A marginal field in offshore Vietnam. *J. Pet. Explor. Prod. Technol.* **2022**, *12*, 1–19. [[CrossRef](#)]
62. Tucker, M.E.; Wright, V.P. *Carbonate Sedimentology*; Blackwells: Oxford, UK, 1990; p. 481.
63. Omidvar, M.; Safari, A.; Vaziri-Moghaddam, H.; Ghalavand, H. Facies analysis and paleoenvironmental reconstruction of Upper Cretaceous sequences in the eastern Para-Tethys Basin, NW Iran. *Geol. Acta* **2014**, *14*, 363–384.
64. Adabi, M.H.; Zohdi, A.; Ghabeishavi, A.; Amiri-Bakhtiyar, H. Applications of nummulitids and other larger benthic foraminifera in depositional environment and sequence stratigraphy: An example from the Eocene deposits in Zagros Basin, SW Iran. *Facies* **2008**, *54*, 499–512. [[CrossRef](#)]
65. Emery, D.; Myers, K. *Sequence Stratigraphy*; John Wiley & Sons: Hoboken, NJ, USA, 2009; p. 264.
66. Duval, B.; Cramez, C.; Vail, P. Types and hierarchy of stratigraphic cycles. *Seq. Stratigr. Eur. Basins* **1992**, *44*.
67. Vail, P.R.; Audemard, F.; Bowman, S.A.; Eisner, P.N.; Perez-Cruz, C. The stratigraphic signatures of tectonics, eustasy and sedimentology—An overview. In *Cycles and Events in Stratigraphy*; Einsele, G., Ricken, W., Seilacher, A., Eds.; Springer: Berlin/Heidelberg, Germany, 1991; pp. 617–659.
68. Catuneanu, O. *Principles of Sequence Stratigraphy*; Elsevier: Amsterdam, The Netherlands, 2006.
69. Posamentier, H.; Jervey, M.T.; Vail, P. Eustatic controls on clastic deposition I—Conceptual framework. *SEPM Spec. Publ.* **1988**, *42*, 125–154.
70. Miall, A.D. *The Geology of Stratigraphic Sequences*; Springer Science & Business Media: New York, NY, USA, 2010.
71. Haq, B.U. Cretaceous eustasy revisited. *Glob. Planet. Change* **2014**, *113*, 44–58. [[CrossRef](#)]
72. Hallam, A. *Phanerozoic Sea-Level Changes*; Columbia University Press: New York, NY, USA, 1992.
73. Arthur, M.; Brumsack, H.-J.; Jenkyns, H.; Schlanger, S. Stratigraphy, geochemistry, and paleoceanography of organic carbon-rich Cretaceous sequences. In *Cretaceous Resources, Events and Rhythms*; Springer: Berlin/Heidelberg, Germany, 1990; pp. 75–119.